Heat and particle transport simulation in COMPASS and T-10 with Canonical Profile Transport Model

A.V. Danilov[1], Yu.N. Dnestrovskij[1], A.V. Melnikov[1,2], S.V. Cherkasov[1], L.G. Eliseev[1], A.Yu. Dnestrovskij[1], S.E. Lysenko[1], G.F. Subbotin[1], V.A. Vershkov[1], J. Havlíček[3], J. Urban[3], J. Stöckel[3], P. Bílková[3], P. Böhm[3], M. Šos[3,4], M. Hron[3], M. Komm[3], R. Pánek[3]

[1]*NRC "Kurchatov Institute", 123182 Kurchatov Sq. 1, Moscow, RF*

[2]*National Research Nuclear University MEPhI, Kashirskoye sh. 31, Moscow, RF*

[3]*Institute of Plasma Physics of the CAS, 18200 Prague 8, CR*

[4] *Faculty of Nuclear Sciences and Physical Engineering, Prague, Břehová 7, CR*

The remarkable property of tokamak plasma to maintain the shape of some parameters profiles (e.g. the electron pressure and temperature, toroidal rotation velocity) under different external influences has been discussed since early eighties [1, 2]. This effect is considered as manifestation of plasma self-organization and provides the basis for the Canonical Profile Transport Model (CPTM) [3]. Despite the large number of observations of this phenomenon, the understanding of its real nature still provides challenge for investigators. In the last decade certain hopes have been connected with zonal flows and their high frequency branch geodesic acoustic mode (GAM). The link between broadband density/potential fluctuations and GAMs has been observed in T-10 [4, 5, 6]. In both COMPASS and T-10, the bicoherence analysis confirmed the nonlinear energy exchange between GAMs and the ambient turbulence [7, 8].

The report presents the CPTM simulation results using the ASTRA code for L-mode plasmas of the circular limiter tokamak T-10 and D-shaped diverted plasmas of COMPASS. On top of that, Ohmic and NBI heated H-mode in COMPASS was modeled. The heat flux in the electron ($\alpha = e$) or ion ($\alpha = i$) channel is presented in the form [9]:

$$q_\alpha = -\chi_\alpha n(T'_\alpha - \frac{T_\alpha}{T_c}T'_c)H(\frac{T'_\alpha}{T_\alpha} - \frac{T'_c}{T_c})F_\alpha - \chi_{0\alpha}nT'_\alpha + 3/2\Gamma_n T_\alpha - \chi_{st}nH(r_s - r)T'_\alpha$$

Here n is the electron density, T_α is electron or ion temperature, T_c is the canonical temperature profile, χ_α is the stiffness of electron or ion temperature profile, $H(x)$ is the Heaviside function, $H(x) = 1$ for $x > 0$, $H(x) = 0$ for $x < 0$. The value $\chi_{0\alpha}$ is the coefficient of thermal conductivity, determined by processes not related to the effect of profile consistency (for example, neoclassical effects). The last two terms describe the convective heat flux,

proportional to the particle flux Γ_n and averaged effect of sawtooth oscillations inside the region $r<r_s$, where $q(r_s)\sim1$.

The particle flux is written as follows:

$$\Gamma_n = nV_w - \frac{D_n}{T_e}(n' - \frac{n}{n_c}n_c')F_e - \frac{D_p}{T_e}(p' - \frac{p}{p_c}p_c')F_e - D_0 n' - D_{st}H(r_s - r)n'$$

The first term in this equation is neoclassical Ware pinch, the next two terms describe the flux driven by electron density and pressure profiles stiffness ($p=p_e=nT_e$) and the last two terms are the "background" particle flux and the flux, connected with sawtooth mixing. Here n_c and p_c are canonical density and pressure profiles.

Both expressions for fluxes contain so called "forgetting factors" F_α [9]:

$$F_\alpha = \exp\{-z_{p\alpha}^2/2z_{0\alpha}^2\}; \qquad z_{p\alpha} = \frac{1}{\rho}\left(\frac{p_\alpha'}{p_\alpha} - \frac{p_c'}{p_c}\right)^{-1}.$$

These factors suppress the fluxes, connected with profile stiffness, inside inner or edge transport barriers, formed in the "forgetting region", where $|z_{p\alpha}|>z_{0\alpha}$. In present paper the stepwise profile of $z_{0\alpha}$ is assumed for H-mode description: $z_{0\alpha}=20$ for $\rho<0.9$ and $z_{0\alpha}=8$ for $0.9<\rho<1$. The value of $z_{0\alpha}$ at the plasma edge is close to those for JET, DIII-D and MAST.

Two COMPASS pulses were chosen for analysis: #9286 and #13652, evolution of some quantities in these discharges is presented in Fig. 1. For both pulses H_α signals provide evidence of long ELM-free high density H-mode, but the pulse #9286 is Ohmic, while in the pulse #13652 the L-H transition occurs at some milliseconds after NBI switch on.

At first, the simulation of Ohmic L-mode phase of the pulse #13652 was performed. For comparison, the T-10 pulse #66022 in Ohmic L-mode was simulated also. The results for electron temperature and density profiles simulation are presented in Fig. 2. The T-10 profiles correspond to the steady phase with plasma current 200 kA and the chord average density $4\cdot10^{19}$ m^{-3}. The Ohmic L-mode simulation enabled to determine the stiffness coefficients D_n and D_p in the particle flux equation. In the case of T-10 these coefficients proved to be about two times less than for COMPASS.

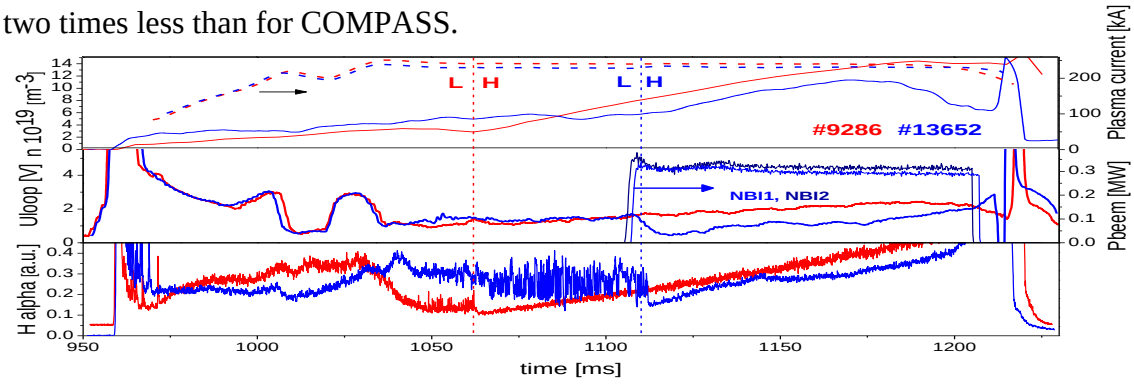

Fig. 1. Plasma current, density, loop voltage, NBI output powers and H_α in COMPASS pulses.

Turning to COMPASS H-mode simulation, we are to set the NBI absorbed power profile in the pulse #13652. The estimation confirms that in the high density H-mode plasma the most part of NBI power is absorbed at the outer half of minor radius. The total absorbed power P_{tot} = 0.35 MW was chosen from the proximity of simulated and measured central electron temperatures. This value is in agreement with the absorbed power estimation to a half of the power in the injector output [10]. As for the effective charge, smooth Z_{eff} values increase during the H-mode phase from 1.5 till 4 – 4.5 was supposed in connection with the impurities accumulation and rather high loop voltage values at the end of H-mode phase.

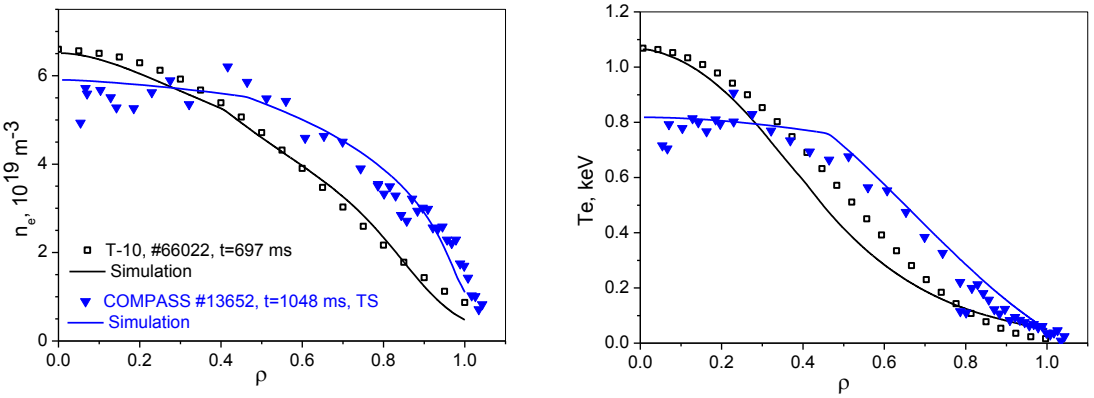

Fig. 2. Plasma density and electron temperature profiles in COMPASS and T-10 Ohmic L-mode.

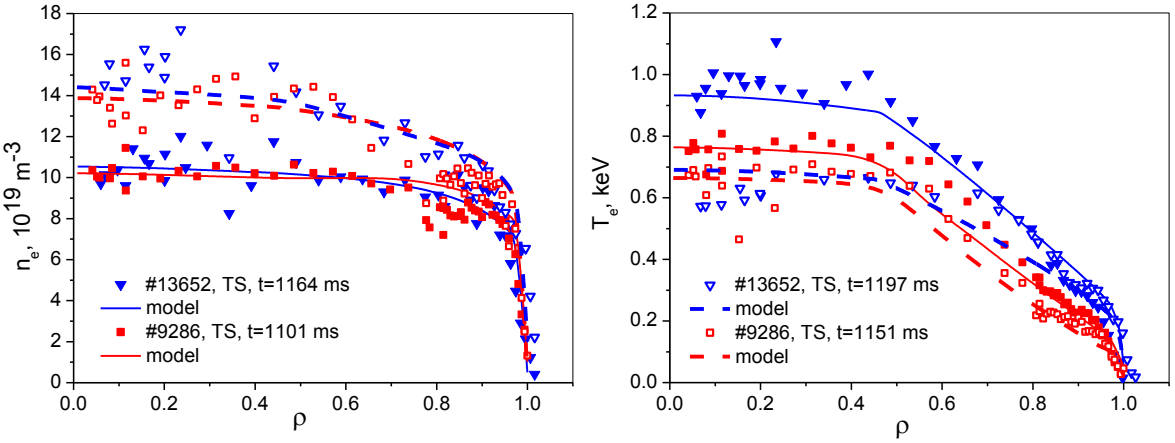

Fig. 3. Comparison of simulated electron density and temperature profiles with TS measurements in COMPASS.

Simulation results for electron temperature and density profiles for two pulses in the H-mode phase are presented in Fig. 3 for two time slices for each pulse. The average plasma densities are close in both pulses at the time moments chosen for profiles comparison. It can be observed that density profiles are quite similar for both pulses, but the electron temperature pedestals are higher for the pulse with NBI heating. Fig. 4 presents the results for the loop voltage and stored energy simulation. One may notice that the loop voltage drop during L-H transition is considerably deeper in the case of NBI heating. Thus the additional NBI power input is partly compensated by Ohmic power decrease and it may be at least one of the

reasons for the similarity of Ohmic and NBI heated H-modes. However, the stored energy increase after the L-H transition is more rapid in the case of NBI heating. All of these features are reproduced during the simulation, but the stored energy is overestimated at the end of H-mode phase. It means that the H-mode degradation due to impurities accumulation is not fully reproduced in simulation.

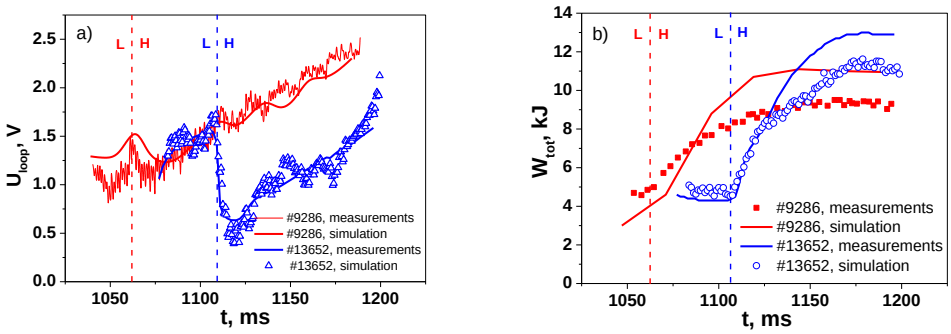

Fig. 4. Comparison of simulated loop voltage (a) and stored energy (b) with measurements.

In conclusion, it can be noted that the possibility of simulating Ohmic L- and H-mode and NBI heated H-mode in COMPASS with Canonical Profile Transport Model is confirmed.

The simulated profiles of plasma density and electron temperature in COMPASS and T-10 Ohmic L-mode are consistent with the measured ones. However, the stiffness coefficients in the particle flux equation for T-10 proved to be about two times less than for COMPASS. In the COMPASS Ohmic and NBI heated H-mode, the density profiles with close average density are similar, while the electron temperature pedestal is higher in the case of NBI heated H-mode and simulated profiles manifest the same features.

Further investigation is to be aimed at the link of canonical profiles and L-H transitions to plasma potential evolution and density fluctuations, as presented in [4] for T-10, or geodesic acoustic mode and Alfvén eigenmodes in COMPASS [7].

The paper is funded by Russian Science Foundation, Project 14-22-00193. The work of authors from the Czech Republic was supported by projects No. CZ.02.1.01/0.0/0.0/16_019/0000768, LM2015045 and GA16-25074S.

[1] Coppi B., *Plasma Phys. Control. Fusion*, 1980, **5**, 261

[2] Kadomtsev B.B., *Sov. J. Plasma Phys.*, 1987, **13,** 443

[3] Dnestrovskij Yu.N., Pereverzev G.V., *Plasma Phys. Control. Fusion*, 1988, **30**, 1417

[4] Vershkov V.A. *et al*, *Nuclear Fusion*, 2015, **55**, 063014

[5] Andreev V.F. *et al*, *Plasma Phys. Control. Fusion*, 2016, **58**, 055008

[6] Melnikov A.V. *et al*, *Plasma Phys. Control. Fusion*, 2006, **48**, 87

[7] Seidl J. *et al*, *Nuclear Fusion*, 2017, **57**, 126048

[8] Melnikov A.V. *et al*, *Nucl. Fusion*, 2017, **57**, 072004

[9] Dnestrovskij Yu.N., Self-Organization of Hot Plasmas, Springer, 2015

[10] Panek R. *et al*, *Proc. 40th EPS Conf. on Plasma Physics*, P4.103, 2013